Nonlinear Backstepping with Time Delay Estimation for Six-Phase Induction Machine

Yassine Kali[1], Jorge Rodas[2], Maarouf Saad[1], Jesus Doval-Gandoy[3] and Raul Gregor[2]
[1]École de Technologie Supérieure, Quebec University, Montreal, QC H3C 1K3, Canada
y.kali88@gmail.com, maarouf.saad@etsmtl.ca
[2]Laboratory of Power and Control Systems, Facultad de Ingeniería, Universidad Nacional de Asunción, Paraguay
jrodas@ing.una.py, rgregor@ing.una.py
[3]Applied Power Electronics Technology Research Group, Universidad de Vigo, Spain, jdoval@uvigo.es

***Abstract*—In this paper, a robust nonlinear stator currents controller based on a known nonlinear technique is proposed for a six-phase induction machine. First of all, a proportional-integral regulator is used in an outer loop to control the speed. Secondly, the inner loop based on a nonlinear method that combines the nonlinear backstepping control scheme with the time delay estimation consists of controlling the stator currents. The chosen time delay estimation method can approximate the unmeasurable rotor current while the nonlinear backstepping can achieve good tracking performances. The stability analysis of the current closed-loop error dynamics is provided based on a recursive Lyapunov function. Numerical simulations have been conducted to demonstrate the efficiency and the performance of the developed nonlinear control method for the asymmetrical six-phase induction machine.**

***Index Terms*—Nonlinear backstepping, time delay estimation, multi-phase induction machine, stator currents control, rotor current estimation, uncertainties, Lyapunov.**

I. Introduction

Nowadays, power electronics, control, machines and drives communities pay a lot of attention to multiphase Induction Machine (IM) drives since they present better features in comparison with classical three-phase IM [1]–[3]. Among these features, we cite lower current/power ratings per phase for the same nominal power, lower torque ripple, improved efficiency and fault tolerant capabilities. For all these reasons, the use of these machines has grown in several fields such as ships, electric vehicles and wind energy generation systems [3], [4]. In power electronics and drives, most of the published works considered the designed methods based on known techniques for three-phase and then extended for multiphase machines [5]–[13]. Nevertheless, robust nonlinear control techniques have been developed for the same topology. The two main used controllers are first and second order sliding mode [14]–[17] and backstepping [18].

Nonetheless, even its good features, the obtained performances using classical sliding mode are affected by the chattering phenomenon that is dangerous for the controlled systems [19]. Moreover, even its ability to reduce or to eliminate the chattering, the implementation of the second order sliding mode is difficult because of the required information that is not always available. Hence, the backstepping method [20] that is also one of the attractive techniques does not suffer from chattering. The aim of this approach is to derive for some system state variables an appropriate stabilization functions based on recursive Lyapunov function candidates. Hence, the stability is ensured at all times. However, the drawback of this method remains on its sensitivity to unknown dynamics and perturbations that can causes several complications during the real-time implementation.

In literature, some works tried to solve this limitation since this problem is common to all existing systems. Thereby, some published papers proposed nonlinear backstepping combined with conventional or second order SMC [21]–[23]. However, these techniques meet the same aforementioned problems, namely, chattering phenomenon and a difficult real-time implementation. Otherwise, the combination of backstepping with fuzzy logic [24], [25] or neural network [26], [27] has been proposed. These last two intelligent techniques are well known for their ability to reproduce a precise estimate of the uncertainties and perturbations. However, the real-time implementation of the introduced fuzzy rules or the large number of parameters still difficult.

To cope with the aforementioned disadvantage, in this paper, the inner stator currents control loop for the asymmetrical six-phase IM drive is based on the nonlinear backstepping method that is combined with Time Delay Estimation (TDE). The proposed approach is simple and robust and has been successfully implemented on a robotic manipulator system [28], [29]. On one hand, without an exact knowledge of the model and based on the time-delayed information of the system's state variables and the input signals, the TDE method [30] can effectively approximate the uncertainties. On the other hand, the resulting TDE error will be rejected by the nonlinear backstepping.

The present paper is divided into five sections. Section II introduces the mathematical model of the asymmetrical six-phase IM while the development of the proposed nonlinear backstepping with TDE method is detailed step by step based on recursive Lyapunov function candidate in Section III. Section IV supports the theoretical part by presenting simulation results and a comparison study with the TDE method based SMC. Finally, some conclusions are drawn in the last section.

This research is funded by the Consejo Nacional de Ciencia y Tecnología (CONACYT) - Paraguay, grant numbers 14-INV-101 and POSG16-05.

II. Model of the Machine and VSI

The studied machine depicted in Fig. 1 consists of an asymmetrical six-phase IM supported by two 3-phase 2-Level Voltage Source Inverter (2L-VSI). The dynamic model of the considered machine is described in state-space representation [15] as follows:

$$\dot{\mathbf{x}}(t) = \mathbf{A}\,\mathbf{x}(t) + \mathbf{B}\,\mathbf{u}(t) + \mathbf{d}(t) \quad (1)$$

$$\mathbf{y}(t) = \mathbf{C}\,\mathbf{x}(t) \quad (2)$$

where $\mathbf{x}(t) = [i_{s\alpha}(t),\, i_{s\beta}(t),\, i_{sx}(t),\, i_{sy}(t), i_{r\alpha}(t),\, i_{r\beta}(t)]^T$ denotes the state vector with $i_{s\alpha}(t)$, $i_{s\beta}(t)$ are the stator current in the $\alpha-\beta$ plane, $i_{sx}(t)$, $i_{sy}(t)$ are the stator current in $x-y$ plane and $i_{r\alpha}(t)$, $i_{r\beta}(t)$ represents the unmeasurable rotor currents, $\mathbf{u}(t) = [u_{s\alpha}(t),\, u_{s\beta}(t),\, u_{sx}(t),\, u_{sy}(t)]^T$ denotes stator input voltages, $\mathbf{y}(t)$ represents the output vector, $\mathbf{d}(t)$ is the (6×1) vector of perturbations due to uncertain parameters and disturbances and the matrices $\mathbf{A}$, $\mathbf{B}$ and $\mathbf{C}$ are given by:

$$\mathbf{A} = \begin{bmatrix} a_{11} & a_{12} & 0 & 0 & a_{15} & a_{16} \\ a_{21} & a_{22} & 0 & 0 & a_{25} & a_{26} \\ 0 & 0 & a_{33} & 0 & 0 & 0 \\ 0 & 0 & 0 & a_{44} & 0 & 0 \\ a_{51} & a_{52} & 0 & 0 & a_{55} & a_{56} \\ a_{61} & A_{62} & 0 & 0 & a_{65} & a_{66} \end{bmatrix} \quad (3)$$

$$\mathbf{B} = \begin{bmatrix} b_{11} & 0 & 0 & 0 \\ 0 & b_{22} & 0 & 0 \\ 0 & 0 & b_{33} & 0 \\ 0 & 0 & 0 & b_{44} \\ b_{51} & 0 & 0 & 0 \\ 0 & b_{62} & 0 & 0 \end{bmatrix} \quad (4)$$

$$\mathbf{C} = \begin{bmatrix} 1 & 0 & 0 & 0 & 0 & 0 \\ 0 & 1 & 0 & 0 & 0 & 0 \\ 0 & 0 & 1 & 0 & 0 & 0 \\ 0 & 0 & 0 & 1 & 0 & 0 \end{bmatrix} \quad (5)$$

The elements of the matrices $\mathbf{A}$ and $\mathbf{B}$ are given in the Appendix. The above model is obtained by using the Vector Space Decomposition (VSD) method. Hence, the $\alpha-\beta$, $x-y$ and the zero-sequence planes are obtained using the decoupling transformation matrix $\mathbf{T}_1$ given by:

$$\mathbf{T}_1 = \frac{1}{3}\begin{bmatrix} 1 & \frac{\sqrt{3}}{2} & -\frac{1}{2} & -\frac{\sqrt{3}}{2} & -\frac{1}{2} & 0 \\ 0 & \frac{1}{2} & \frac{\sqrt{3}}{2} & \frac{1}{2} & -\frac{\sqrt{3}}{2} & -1 \\ 1 & -\frac{\sqrt{3}}{2} & -\frac{1}{2} & \frac{\sqrt{3}}{2} & -\frac{1}{2} & 0 \\ 0 & \frac{1}{2} & -\frac{\sqrt{3}}{2} & \frac{1}{2} & \frac{\sqrt{3}}{2} & -1 \\ 1 & 0 & 1 & 0 & 1 & 0 \\ 0 & 1 & 0 & 1 & 0 & 1 \end{bmatrix} \quad (6)$$

Moreover, the rotor speed $\omega_r(t)$ is defined as follows:

$$\begin{aligned} \dot{\omega}_r(t) &= -\frac{B_M}{J_M}\,\omega_r(t) + \frac{P}{J_M}\,(T_e(t) - T_l(t)) \\ T_e(t) &= 3\,P\,(\psi_{s\alpha}(t)\,i_{s\beta}(t) - \psi_{s\beta}(t)\,i_{s\alpha}(t)) \end{aligned} \quad (7)$$

where T_e and T_l denote respectively the generated torque and the load torque, P represents the number of pole pairs, J_M and B_M denote respectively the coefficients of inertia and friction, $\psi_{s\alpha}(t)$ and $\psi_{s\beta}(t)$ are the stator fluxes.

Furthermore, the stator voltages are related to the VSI model by the following formula:

$$V_{\rm dc}\,\mathbf{T}_1\,\mathbf{M} = [u_{s\alpha}(t),\, u_{s\beta}(t),\, u_{sx}(t),\, u_{sy}(t)]^T \quad (8)$$

where $V_{\rm dc}$ represents the DC-bus voltage and the VSI model is defined by:

$$\mathbf{M} = \frac{1}{3}\begin{bmatrix} 2 & 0 & -1 & 0 & -1 & 0 \\ 0 & 2 & 0 & -1 & 0 & -1 \\ -1 & 0 & 2 & 0 & -1 & 0 \\ 0 & -1 & 0 & 2 & 0 & -1 \\ -1 & 0 & -1 & 0 & 2 & 0 \\ 0 & -1 & 0 & -1 & 0 & 2 \end{bmatrix}\mathbf{S}^T \quad (9)$$

where $\mathbf{S} = [S_a,\, S_b,\, S_c,\, S_d,\, S_e,\, S_f]$ denotes the the gating signals vector such as $S_i \in \{0, 1\}$.

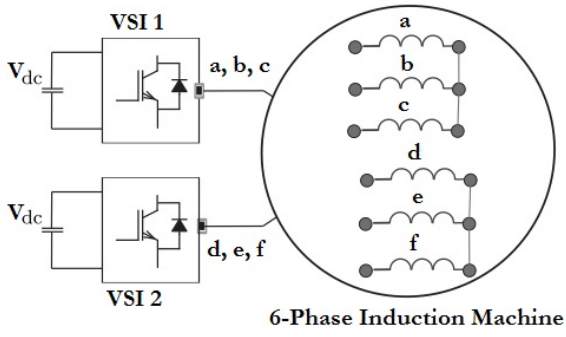

Fig. 1. Scheme of the 6-phase IM supported by two 3-phase 2L-VSI

III. Controller Design

Let us select the desired stator currents trajectories vector as $\mathbf{y}^*(t) = \left[i^*_{s\alpha}(t),\, i^*_{s\beta}(t),\, i^*_{sx}(t),\, i^*_{sy}(t)\right]^T$ and the tracking error vector as $\tilde{\mathbf{y}}(t) = \mathbf{y}(t) - \mathbf{y}^*(t)$, the purpose is to develop a robust nonlinear control vector $\mathbf{u}(t)$ that ensures the convergence of $\tilde{\mathbf{y}}(t)$ to zero and robustness against perturbations and unknown dynamics (unmeasurable rotor current). To that end, an outer and inner control loops will be designed. On one hand, based on IRFOC, the outer loop consists of a PI regulator to control the speed. The output of this loop will provide the current reference $i^*_{sq}(t)$. Then, the desired stator current in $\alpha-\beta$ plane is generated by choosing a desired $i^*_{sq}(t)$ and using Park's transformation. On the other hand, the inner loop will use a TDE method based nonlinear backstepping to control the stator currents. The block diagram of the closed-loop system is depicted in Fig. 2.

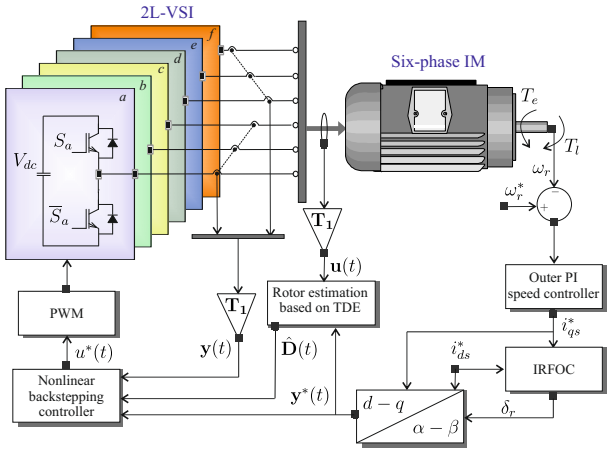

Fig. 2. Block diagram of the proposed control scheme.

The first step in the design procedure is to select the vector of tracking error $\tilde{\mathbf{y}}(t)$ as a regulated variable. Computing its first time derivative yields to:

$$\begin{aligned}\dot{\tilde{\mathbf{y}}}(t) &= \dot{\mathbf{y}}(t) - \dot{\mathbf{y}}^*(t)\\ &= \mathbf{C}\,\dot{\mathbf{x}}(t) - \dot{\mathbf{y}}^*(t)\\ &= \mathbf{C}\,\mathbf{A}\,\mathbf{x}(t) + \mathbf{C}\,\mathbf{B}\,\mathbf{u}(t) + \mathbf{C}\,\mathbf{d}(t) - \dot{\mathbf{y}}^*(t)\\ &= \mathbf{A}_1\,\mathbf{y}(t) + \mathbf{B}_1\,\mathbf{u}(t) + \mathbf{D}(t) - \dot{\mathbf{y}}^*(t)\end{aligned} \tag{10}$$

where $\mathbf{A}_1$, $\mathbf{B}_1$ and $\mathbf{D}(t)$ are defined by:

$$\mathbf{A}_1 = \begin{bmatrix} a_{11} & a_{12} & 0 & 0\\ a_{21} & a_{22} & 0 & 0\\ 0 & 0 & a_{33} & 0\\ 0 & 0 & 0 & a_{44}\end{bmatrix} \tag{11}$$

$$\mathbf{B}_1 = \begin{bmatrix} b_{11} & 0 & 0 & 0\\ 0 & b_{22} & 0 & 0\\ 0 & 0 & b_{33} & 0\\ 0 & 0 & 0 & b_{44}\end{bmatrix} \tag{12}$$

$$\mathbf{D}(t) = \begin{bmatrix} d_1(t) + A_{15}\,\mathbf{x}_5(t) + A_{16}\,\mathbf{x}_6(t)\\ d_2(t) + A_{25}\,\mathbf{x}_5(t) + A_{26}\,\mathbf{x}_6(t)\\ d_3(t)\\ d_4(t)\end{bmatrix} \tag{13}$$

In order to reach our goal (make the error $\tilde{\mathbf{y}}(t)$ converge to zero), a control will be derived by selecting the following Lyapunov function:

$$\mathbf{V}(t) = \frac{1}{2}\tilde{\mathbf{y}}^T(t)\,\tilde{\mathbf{y}}(t) + \frac{1}{2}\epsilon^T(t)\,\Gamma\,\epsilon(t) \tag{14}$$

where $\Gamma \in R^{4\times4}$ is diagonal matrix with strictly positive elements and $\epsilon(t) = \mathbf{D}(t) - \hat{\mathbf{D}}(t)$ is the vector of estimation error with $\hat{\mathbf{D}}(t)$ is the estimate vector of $\mathbf{D}(t)$ that will be determinate later. Computing the first time derivative of $\mathbf{V}(t)$ gives:

$$\begin{aligned}\dot{\mathbf{V}}(t) =& \tilde{\mathbf{y}}^T(t)\,\dot{\tilde{y}}(t) + \epsilon^T(t)\,\Gamma\,\dot{\epsilon}(t)\\ =& \tilde{\mathbf{y}}^T(t)\,[\mathbf{A}_1\,\mathbf{y}(t) + \mathbf{B}_1\,\mathbf{u}(t) + \mathbf{D}(t) - \dot{\mathbf{y}}^*(t)]\\ &+ \epsilon^T(t)\,\Gamma\,\dot{\epsilon}(t)\end{aligned} \tag{15}$$

Selecting the following control law:

$$\mathbf{u}(t) = \mathbf{B}_1^{-1}\left[\dot{\mathbf{y}}^*(t) - \mathbf{A}_1\,\mathbf{y}(t) - \hat{\mathbf{D}}(t) - K\,\tilde{\mathbf{y}}(t)\right] \tag{16}$$

where $K \in R^{4\times4}$ is a diagonal positive matrix. Hence, substituting the above controller in $\dot{\mathbf{V}}(t)$ yields to:

$$\begin{aligned}\dot{\mathbf{V}}(t) =& \tilde{\mathbf{y}}^T(t)\left[\mathbf{D}(t) - \hat{\mathbf{D}}(t) - K\,\tilde{\mathbf{y}}(t)\right] + \epsilon^T(t)\,\Gamma\,\dot{\epsilon}(t)\\ =& -\tilde{\mathbf{y}}^T(t)\,K\,\tilde{\mathbf{y}}(t) + \epsilon^T(t)\,[\tilde{\mathbf{y}}(t) + \Gamma\,\dot{\epsilon}(t)]\end{aligned} \tag{17}$$

To ensure that the above equation is negative definite, the following condition must be met:

$$\tilde{\mathbf{y}}(t) + \Gamma\,\dot{\epsilon}(t) = 0 \tag{18}$$

Developing (18) gives:

$$\hat{\mathbf{D}}(t) = \mathbf{D}(t) + L\,\Gamma^{-1}\,\tilde{\mathbf{y}}(t) \tag{19}$$

Assuming that the uncertain vector is continuous and differentiable and slow varying between two very close time period such as $\mathbf{D}(t) \cong \mathbf{D}(t-L)$. Then, the term $\hat{\mathbf{D}}(t)$ can be obtained using TDE as follows:

$$\begin{aligned}\hat{\mathbf{D}}(t) &= \mathbf{D}(t-L) + L\,\Gamma^{-1}\,\tilde{\mathbf{y}}(t)\\ &= \dot{\mathbf{y}}(t-L) - \mathbf{A}_1\,\mathbf{y}(t-L) - \mathbf{B}_1\,\mathbf{u}(t-L) + L\Gamma^{-1}\tilde{\mathbf{y}}(t)\end{aligned} \tag{20}$$

where L represents the delay that is usually selected to be equal to the sampling period.

Hence, substituting (16) and (20) in $\dot{\mathbf{V}}(t)$ gives:

$$\dot{\mathbf{V}}(t) = -\tilde{\mathbf{y}}^T(t)\,K\,\tilde{\mathbf{y}}(t) \leq -\lambda_{min}(K)\|\tilde{\mathbf{y}}(t)\|^2 \tag{21}$$

where $\lambda_{min}(K)$ is the minimum eigenvalue of K. Hence, the closed-loop system is stable.

IV. Numerical Simulation

In this part, a simulation program using MATLAB/Simulink has been carried out to prove the efficiency of the developed controller for the considered asymmetrical six-phase IM. The mechanical and electrical parameters of the considered machine can be found in [15] and in the Appendix. To perform this simulation, the sampling frequency is chosen to be $f = 10$ kHz while the delay L is selected to be $1/f$, the torque load connected to the asymmetrical six-phase IM is selected to be 2 N.m and the imposed d current has been fixed at ($i^*_{sd} = 1$ A). For the outer speed control loop, the PI regulator gains are chosen as follows:

$$K_p = 9.17,\ K_I = 0.027.$$

In this part, the performance of the proposed backstepping with TDE will be quantified by a comparative study with the proposed SMC combined to TDE in [14], [15], [31] based on the Mean Squared Error (MSE) between the measured currents and their respective references and on the Total Harmonic Distortion (THD) in the $\alpha-\beta$ plane. These two indices are defined by:

$$\begin{aligned}\mathrm{MSE}(\mathbf{y}_i) &= \sqrt{\frac{1}{N}\sum_{k=1}^{N}\tilde{\mathbf{y}}_i^2(k)}\\ \mathrm{THD}(\mathbf{y}_i) &= \sqrt{\frac{1}{i_{s1}}\sum_{j=2}^{N} i_{sj}^2}\end{aligned} \tag{22}$$

where N represents the total number of simulation samples, i_{s1} and i_{sj} represent respectively the fundamental and the harmonic stator currents.

A. Results obtained via the proposed backstepping with TDE

The proposed control law described in the previous section is given in (16). During the simulation, the gains of the inner control loop are chosen as follows:

$$K = \text{diag}(500, 500, 200, 200),$$

$$\Gamma = \text{diag}(0.1, 0.1, 0.1, 0.1).$$

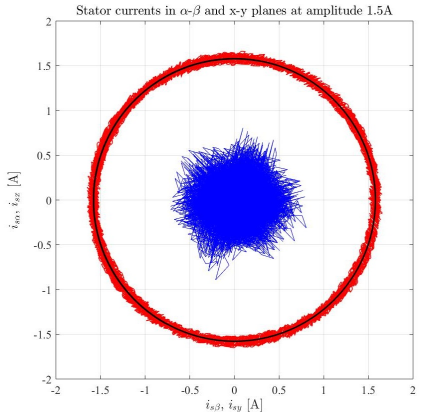

(a)

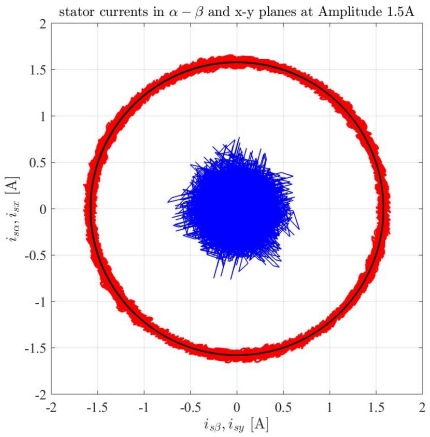

(b)

Fig. 3. Stator currents tracking in $\alpha-\beta$ and $x-y$ planes: (a) Results obtained via the proposed approach, (b) Results obtained via SMC with TDE.

For an $i^*_{s\alpha\beta}$ amplitude of 1.5 A, Fig. 3(a) shows the response of the output vector. Moreover, Fig. 4(a) shows that the stator currents in $\alpha-\beta$ plane track precisely their desired references in the transient and the steady-state of the desired rotor speed. Finally, the behavior of the control input signals are depicted in Fig. 5(a).

B. Results obtained via SMC with TDE

A complete study of this method can be found in [15], [32]. The control law for the considered asymmetrical six-phase IM is obtained as follows:

$$\begin{aligned}\mathbf{u}(t) =& \mathbf{B}_1^{-1}\left[-\mathbf{A}_1\,\mathbf{y}(t) + \dot{\mathbf{y}}^*(t) + \mathbf{B}_1\,\mathbf{u}(t-L)\cdots\right.\\ &\left.\cdots - \dot{\mathbf{y}}(t-L) + \mathbf{A}_1\,\mathbf{y}(t-L) - \eta\,\text{sgn}(\tilde{\mathbf{y}}(t))\right]\end{aligned} \tag{23}$$

where η is a (4×4) diagonal positive matrix chosen to be $\text{diag}(30, 30, 30, 30)$ such as the convergence and the closed-loop stability are guaranteed in finite-time and $\text{sgn}(\tilde{\mathbf{y}}(t)) = [\text{sgn}(\tilde{\mathbf{y}}_1(t)), \cdots, \text{sgn}(\tilde{\mathbf{y}}_4(t))]^T$ such as $\text{sgn}(\tilde{\mathbf{y}}_i(t))$ for $i = 1, \cdots, 4$ is defined as follows:

$$\text{sgn}(\tilde{\mathbf{y}}_i(t)) = \begin{cases} 1, & \text{if } \tilde{\mathbf{y}}_i(t) > 0 \\ 0, & \text{if } \tilde{\mathbf{y}}_i(t) = 0 \\ -1, & \text{if } \tilde{\mathbf{y}}_i(t) < 0 \end{cases} \tag{24}$$

The simulation results in Fig. 4(b) shows the effectiveness of this nonlinear technique thanks to the convergence of the controlled stator currents in finite-time to their desired trajectories even in the presence of unknown dynamics. However, this method still suffering from the main disadvantage of the conventional SMC which is the chattering as depicted in Fig. 5(b).

C. Discussion

The results of the comparative study are summarized in Table I. Based on this quantitative comparison and on the behavior of tracking and control inputs, the proposed method shows its superiority such that the performances obtained are quite similar while the problem of chattering and the control effort are greatly reduced, especially for the stator current in $x-y$ plane. This amelioration makes the proposed controller more attractive since the generated control inputs are less dangerous than the ones obtained using SMC with TDE that could damage the motor.

TABLE I
COMPARATIVE STUDY IN TERM OF MSE AND THD OF THE STATOR CURRENTS

	Proposed method	SMC with TDE
MSE($\mathbf{y}_1$)	0.0311	0.0325
MSE($\mathbf{y}_2$)	0.0309	0.0318
MSE($\mathbf{y}_3$)	0.1942	0.01678
MSE($\mathbf{y}_4$)	0.2118	0.01861
THD($\mathbf{y}_1$)	23.61	23.55
THD($\mathbf{y}_2$)	23.71	23.65

V. CONCLUSION

A robust nonlinear backstepping control with TDE method has been proposed in this work for stator currents tracking in the $\alpha-\beta$ and $x-y$ planes. On the one hand, highly precise approximation of the perturbations and the unmeasurable rotor current has been enabled in a simple way via the TDE method. On the other hand, backstepping scheme rejects the effect of the nonlinearities caused by TDE error and ensures that the output vector tracks with high accuracy the known desired vector of currents. The efficiency of the developed technique has been supported by the results of Matlab/Simulink simulations on an asymmetrical six-phase IM. The results showed that the proposed approach allows high performances and provides better results in comparison with the combined sliding mode with time delay estimation.

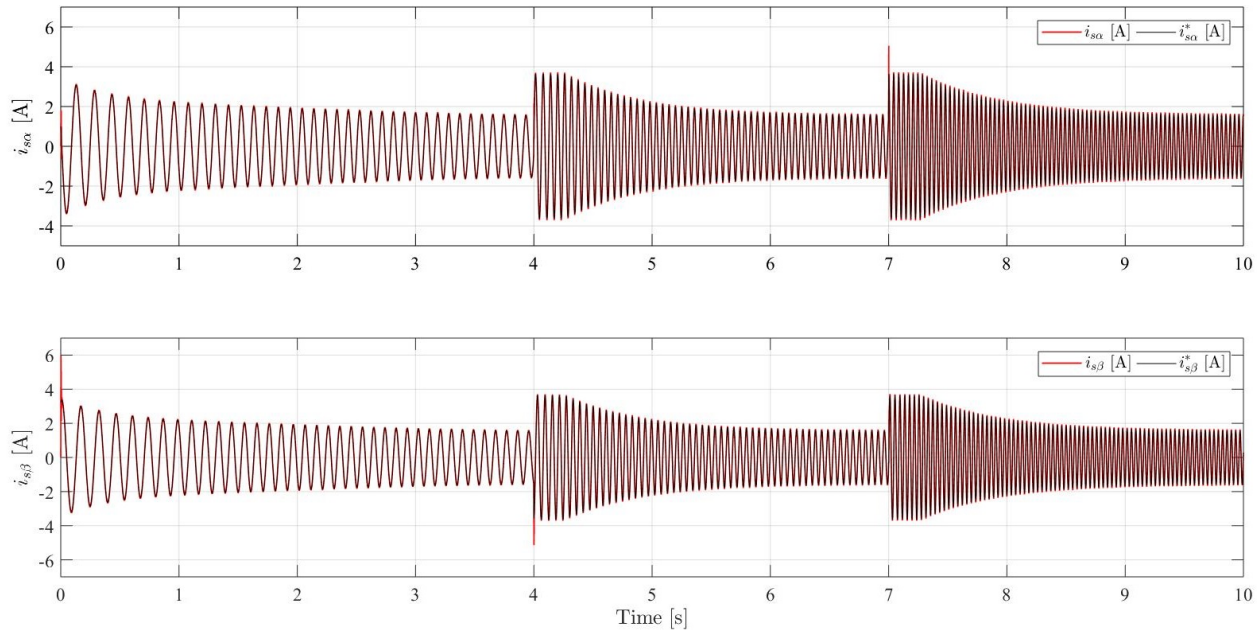

(a)

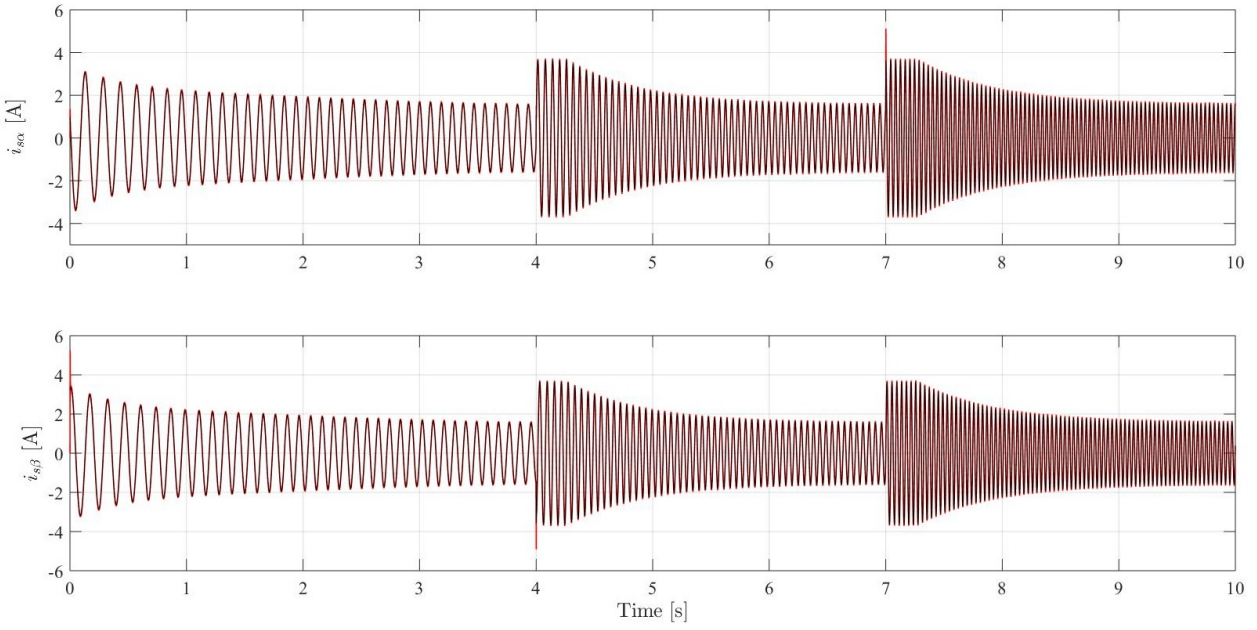

(b)

Fig. 4. Stator currents tracking in $\alpha - \beta$ plane for a fixed rotor speed: (a) Results obtained via the proposed approach, (b) Results obtained via SMC with TDE.

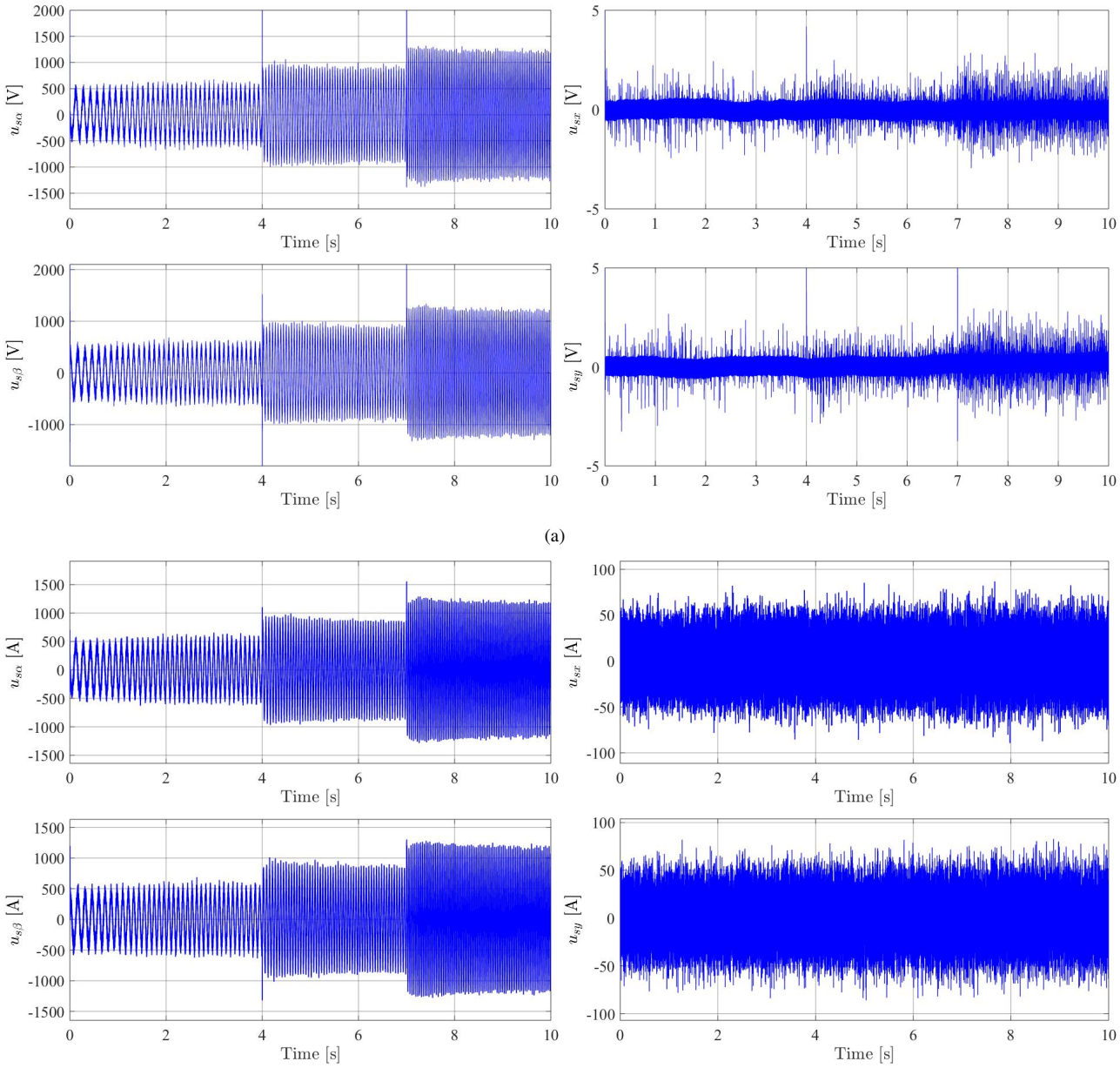

Fig. 5. Control input signals for stator currents: (a) Results obtained via the proposed approach, (b) Results obtained via SMC with TDE.

APPENDIX

The element of the matrices in (3) and (4) are defined as follows:

$$a_{11} = a_{22} = -\frac{L_r R_s}{L_s L_r - L_m^2}$$
$$a_{12} = -a_{21} = \frac{L_m^2}{L_s L_r - L_m^2}\,\omega_r(t)$$
$$a_{15} = a_{26} = \frac{L_m R_r}{L_s L_r - L_m^2}$$
$$a_{16} = -a_{25} = \frac{L_m L_r}{L_s L_r - L_m^2}\,\omega_r(t)$$
$$a_{33} = a_{44} = -\frac{R_s}{L_{ls}}$$
$$a_{51} = a_{62} = \frac{L_m R_s}{L_s L_r - L_m^2}$$
$$a_{52} = -a_{61} = -\frac{L_s L_m}{L_s L_r - L_m^2}\,\omega_r(t)$$
$$a_{55} = a_{66} = -\frac{L_s R_r}{L_s L_r - L_m^2}$$
$$a_{56} = -a_{65} = -\frac{L_s L_r}{L_s L_r - L_m^2}\,\omega_r(t)$$
$$b_{11} = b_{22} = \frac{L_r}{L_s L_r - L_m^2}$$
$$b_{33} = b_{44} = \frac{1}{L_{ls}}$$
$$b_{51} = b_{62} = -\frac{L_m}{L_s L_r - L_m^2}$$

where L_m is the magnetizing inductance, L_{lr} and L_{ls} denote respectively the leakage inductance of the rotor and stator, $L_r = L_{lr} + L_m$ and $L_s = L_{ls} + L_m$ denote respectively the inductance of the rotor and stator, R_r and R_s denote respectively the resistance of the rotor and stator and $\omega_r(t)$ represents the rotor electrical speed. The above parameters are given in Table II.

TABLE II
ELECTRICAL AND MECHANICAL PARAMETERS OF THE SIX-PHASE IM

Parameter	Value	Parameter	Value
R_r	6.9 Ω	L_s	654.4 mH
R_s	6.7 Ω	P	1
L_{ls}	5.3 mH	B_i	0.0004 kg.m^2/s
L_{lr}	12.8 mH	J_i	0.07 kg.m^2
L_r	626.8 mH	Nominal Power	2 kW
L_m	614 mH	Nominal Speed	3000 rpm

REFERENCES

[1] F. Barrero and M. J. Duran, "Recent advances in the design, modeling, and control of multiphase machines: Part I," *IEEE Trans. Ind. Electron.*, vol. 63, no. 1, pp. 449–458, 2016.

[2] M. J. Duran and F. Barrero, "Recent advances in the design, modeling, and control of multiphase machines: Part II," *IEEE Trans. Ind. Electron.*, vol. 63, no. 1, pp. 459–468, 2016.

[3] E. Levi, "Advances in converter control and innovative exploitation of additional degrees of freedom for multiphase machines," *IEEE Trans. Ind. Electron.*, vol. 63, no. 1, pp. 433–448, 2016.

[4] I. Zoric, M. Jones, and E. Levi, "Arbitrary power sharing among three-phase winding sets of multiphase machines," *IEEE Trans. Ind. Electron.*, vol. 65, no. 2, pp. 1128–1139, 2018.

[5] R. Gregor and J. Rodas, "Speed sensorless control of dual three-phase induction machine based on a Luenberger observer for rotor current estimation," in *Proc. IEEE IECON*, 2012, pp. 3653–3658.

[6] A. G. Yepes, J. Malvar, A. Vidal, O. López, and J. Doval-Gandoy, "Current harmonics compensation based on multiresonant control in synchronous frames for symmetrical n-phase machines," *IEEE Trans. Ind. Electron.*, vol. 62, no. 5, pp. 2708–2720, 2015.

[7] M. Ayala, O. Gonzalez, J. Rodas, R. Gregor, and J. Doval-Gandoy, "A speed-sensorless predictive current control of multiphase induction machines using a Kalman filter for rotor current estimator," in *Proc. ESARS-ITEC*, 2016, pp. 1–6.

[8] J. Rodas, F. Barrero, M. R. Arahal, C. Martín, and R. Gregor, "Online estimation of rotor variables in predictive current controllers: a case study using five-phase induction machines," *IEEE Trans. Ind. Electron.*, vol. 63, no. 9, pp. 5348–5356, 2016.

[9] J. Rodas, C. Martín, M. R. Arahal, F. Barrero, and R. Gregor, "Influence of covariance-based ALS methods in the performance of predictive controllers with rotor current estimation," *IEEE Trans. Ind. Electron.*, vol. 64, no. 4, pp. 2602–2607, 2017.

[10] O. Gonzlez, J. Rodas, M. Ayala, R. Gregor, M. Rivera, M. J. Duran, and I. Gonzalez-Prieto, "Predictive current control with kalman filter observer for a five-phase induction machine operating at fixed switching frequency," in *Proc. IEEE ICIEA*, 2017, pp. 349–354.

[11] O. Gonzlez, J. Rodas, R. Gregor, M. Ayala, and M. Rivera, "Speed sensorless predictive current control of a five-phase induction machine," in *Proc. IEEE ICIEA*, 2017, pp. 343–348.

[12] J. Rodas, H. Guzman, R. Gregor, and B. Barrero, "Model predictive current controller using Kalman filter for fault-tolerant five-phase wind energy conversion systems," in *7th International Symposium on Power Electronics for Distributed Generation Systems (PEDG)*, 2016, pp. 1–6.

[13] O. Gonzalez, M. Ayala, J. Rodas, R. Gregor, G. Rivas, and J. Doval-Gandoy, "Variable-speed control of a six-phase induction machine using predictive-fixed switching frequency current control techniques," in *Proc. IEEE PEDG*, 2018, pp. 1–6.

[14] M. Ayala, O. Gonzalez, J. Rodas, R. Gregor, Y. Kali, and P. Wheeler, "Comparative study of non-linear controllers applied to a six-phase induction machine," in *Proc. ESARS-ITEC*, 2018, pp. 1–6.

[15] Y. Kali, M. Ayala, J. Rodas, M. Saad, J. Doval-Gandoy, R. Gregor, and K. Benjelloun, "Current control of a six-phase induction machine drive based on discrete-time sliding mode with time delay estimation," *Energies*, vol. 12, no. 1, 2019. [Online]. Available: http://www.mdpi.com/1996-1073/12/1/170

[16] Y. Kali, J. Rodas, M. Saad, R. Gregor, K. Bejelloun, and J. Doval-Gandoy, "Current control based on super-twisting algorithm with time delay estimation for a five-phase induction motor drive," in *Proc. IEMDC*, 2017, pp. 1–8.

[17] Y. Kali, J. Rodas, M. Saad, R. Gregor, K. Bejelloun, J. Doval-Gandoy, and G. Goodwin, "Speed control of a five-phase induction motor drive using modified super-twisting algorithm," in *Proc. SPEEDAM*, 2018, pp. 938–943.

[18] H. Echeikh, R. Trabelsi, M. F. Mimouni, A. Iqbal, and R. Alammari, "High performance backstepping control of a five phase induction motor drive," in *Proc. ISIE*, June 2014, pp. 812–817.

[19] I. Boiko and L. Fridman, "Analysis of chattering in continuous sliding-mode controllers," *IEEE Trans. Autom. Control*, vol. 50, pp. 1442–1446, 2005.

[20] J. Slotine and W. Li, *Applied nonlinear control*. Printice-Hall international, 1991.

[21] G. Bartolini, A. Ferrara, L. Giacomini, and E. Usai, "A combined backstepping/second order sliding mode approach to control a class of nonlinear systems," in *Proc. VSS*, Dec 1996, pp. 205–210.

[22] N. Adhikary and C. Mahanta, "Integral backstepping sliding mode control for underactuated systems: Swing-up and stabilization of the cartpendulum system," *ISA Trans.*, vol. 52, no. 6, pp. 870 – 880, 2013.

[23] Y. Kali, M. Saad, and K. Benjelloun, *Control of Robot Manipulators Using Modified Backstepping Sliding Mode*. Singapore: Springer Singapore, 2019, pp. 107–136.

[24] S. Jagannathan and F. Lewis, "Robust backstepping control of a class of nonlinear systems using fuzzy logic," *Information Sciences*, vol. 123, no. 3, pp. 223 – 240, 2000.

[25] L. Chunhui and W. Lei, "Backstepping adaptive fuzzy control for a class of nonlinear systems," in *Proc. CCDC*, May 2017, pp. 644–649.

[26] C. Kwan and F. L. Lewis, "Robust backstepping control of nonlinear systems using neural networks," *IEEE Trans. Syst. Man Cybern. A Syst. Hum.*, vol. 30, no. 6, pp. 753–766, Nov 2000.

[27] X. Cao, P. Shi, Z. Li, and M. Liu, "Neural-network-based adaptive backstepping control with application to spacecraft attitude regulation," *IEEE Trans. Neural Netw. Learn. Syst.*, vol. 29, no. 9, pp. 4303–4313, 2018.

[28] Y. Kali, M. Saad, K. Benjelloun, and M. Benbrahim, "Control of uncertain robot manipulators using integral backstepping and time delay estimation," in *Proc. ICINCO*, 2016, pp. 145–151.

[29] Y. Kali, M. Saad, J.-P. Kenné, and K. Benjelloun, *Robot Manipulator Control Using Backstepping with Lagrange's Extrapolation and PI Compensator*. Singapore: Springer Singapore, 2019, pp. 137–161.

[30] K. Youcef-Toumi and O. Ito, "A time delay controller for systems with unknown dynamics," *ASME J. Dyn. Syst. Meas. Control*, vol. 112, pp. 133–141, 1990.

[31] Y. Kali, J. Rodas, M. Ayala, M. Saad, R. Gregor, K. Benjelloun, J. Doval-Gandoy, and G. Goodwin, "Discrete-time sliding mode with time delay estimation of a six-phase induction motor drive," in *Proc. IEEE IECON*, 2018, pp. 5807–5812.

[32] Y. Kali, M. Saad, K. Benjelloun, and M. Benbrahim, "Sliding mode with time delay control for MIMO nonlinear systems with unknown dynamics," in *Proc. RASM*, 2015, pp. 1–6.